Cross-spectral analysis of tremor time series

J. Timmer[1], M. Lauk[1], B. Köster[2], B. Hellwig[2], S. Häußler[1,2]
B. Guschlbauer[2], V. Radt [1], M. Eichler [3], G. Deuschl [4], C.H. Lücking[2]

[1]Zentrum für Datenanalyse und Modellbildung
and Department of Physics, University of Freiburg
Eckerstr. 1, 79104 Freiburg, Germany
[2]Department of Neurology and Clinical Neurophysiology,
University of Freiburg, Breisacher Str. 64, 79110 Freiburg, Germany
[3]Institute for Applied Mathematics, University of Heidelberg,
Im Neuenheimer Feld 294, Germany
[4] Department of Neurology, University of Kiel,
Niemannsweg 147, 24105 Kiel, Germany

October 27, 1999

Running title: Cross-spectral analysis of tremor time series
Keywords: Cross-spectral analysis; Graphical models; Time series analysis; Biomedical data; Hypothesis testing; Tremor.
Address correspondence to:
J. Timmer, FDM, Universität Freiburg, Eckerstr. 1, 79104 Freiburg, Germany. Tel.: +49 761 203-5829, Fax: +49 761 203-7700
email: jeti@fdm.uni-freiburg.de

Abstract

We discuss cross-spectral analysis and report applications for the investigation of human tremors. For the physiological tremor in healthy subjects, the analysis enables to determine the resonant contribution to the oscillation and allows to test for a contribution of reflexes to this tremor. Comparing the analysis of the relation between the tremor of both hands in normal subjects and subjects with a rare abnormal organization of certain neural pathways proves the involvement of central structures in enhanced physiological tremor. The relation between the left and the right side of the body in pathological tremor shows a specific difference between orthostatic and all other forms of tremor. An investigation of EEG and tremor in patients suffering from Parkinson's disease reveals the tremor-correlated cortical activity. Finally, the general issue of interpreting the results of methods designed for the analysis of bivariate processes when applied to multivariate processes is considered. We discuss and apply partial cross-spectral analysis in the frame of graphical models as an extention of bivariate cross-spectral analysis for the multivariate case.

1 Introduction

Since many decades the electrophysiological and mathematical analysis of human tremor was subject to numerous studies. Tremor is defined as the involuntary, oscillatory movement of parts of the body, mainly the upper limbs (15). There are different kinds of tremor, differentiated by clinical criteria. The better understanding of the generating mechanisms of the different human tremors could lead to an improvement of diagnosis and therapy of tremor diseases. Although the most common types of tremor, physiological tremor, enhanced physiological tremor, essential tremor and Parkinsonian tremor, were subject to numerous studies, their mechanisms and origins are still unknown, for reviews see, e.g. (20; 18; 17).

Shortly, the physiological tremor denotes a fine, low-amplitude mostly invisible oscillatory movement of the outstretched hand and is present more or less intense in all humans. Its origin is still under discussion. It was supposed to originate from reflex loops (41; 67; 1), by random synchronization (9) or from a central oscillator (42; 34; 61). The frequency of physiological tremor usually ranges from 7 Hz up to 11 Hz and depends on the weight of the hand, i.e. its frequency decreases if the outstretched hand is loaded with weights (17). The so called enhanced physiological tremor denotes a tremor whose frequency also depends on the load of the hand but with a pathological tremor amplitude. Prominent examples are the tremor caused by drug abuse, by excitement or by fear.

Essential tremor is a hereditary form of tremor and the most common pathological tremor. Its frequency usually ranges from 4.5 Hz up to 10 Hz (17). Parkinsonian tremor is the second most common form of all pathological tremors. Its frequency usually ranges from 4 Hz up to 8 Hz (17). It is one of the prominent symptoms of Parkinson's Disease. The so-called orthostatic tremor was supposed to be a special kind of essential tremor (65; 10; 44; 7) that only occurs during standing and shows an unusual high frequency around 15 Hz. However, recent observations suggest that orthostatic tremor is a separate from of tremor (35; 36). Although frequencies and amplitudes can differ substantially, they are not sufficient criteria for a reliable diagnosis of different pathological forms of tremor (20; 17; 43).

Cross-spectral methods provide a powerful tool to investigate the relation between simultaneously recorded signals. These methods have been used in tremor research to study the relation between muscle activity (electromyogram (EMG)) and magnetoencephalogram (MEG) (64; 54), between EMG and electroencephalogramm (EEG) (32; 51; 27), between EMGs and mechanical measurements (23; 45; 21; 52; 53; 1; 31; 46; 62; 61), between EMGs (19; 3; 36) and between single units and EMGs (21; 40; 39).

In this paper we describe the benefits and limits of cross-spectral analysis in different "real-world" problems in tremor research. Section 2 describes the data recordings and gives a brief overview of the mathematical fundamentals of cross-spectral analysis, estimation procedures and partial cross-spectral analysis. In Sec. 3.1 we address the contribution of reflexes to physiological tremor, in Sec. 3.2 we discuss the involvement of central structures in the generation of physiological tremor. Section 3.3 develops a diagnosis criterion for orthostatic tremor by the use of cross-spectral methods. Sec. 3.4 describes the cross-spectral analysis of EEG and tremor time series in Parkinsonian patients detecting the tremor correlated cortical activity. Furthermore, cortical signal transmission pathways in a healthy subject are identified by partial cross-spectral analysis.

2 Methods

2.1 Recording Techniques

In the application section below we analyze three different kinds of time series: 1) Accelerometer signals representing the mechanical movements of the hand, 2) surface electromyogram (EMG) representing the muscle activity as a difference of potential between two electrodes placed on the skin over the respective muscle and 3) electroencephalogram (EEG) representing the cortical activity as potential measured over the scalp of a subject. To give an impression Fig. 1 shows three arbitrary clippings of a patient suffering from Parkinson's disease.

Fig. 1 around here

During the recording, subjects were sitting in a comfortable, heavy chair with their arms supported. The forearms were fixed proximal of the wrist with a strap. To measure the postural tremor, subjects were asked to hold their hands outstretched in pronated position and to avoid any voluntary movement. For the resting tremor measurements, subjects were asked to avoid any voluntary muscle contraction or movement of their hands. The duration of each record was 30 s. Hand acceleration (ACC) was recorded by light weight piezoresistive accelerometers attached to the belly of the right and left hand (16; 58). Surface EMGs were recorded from the wrist flexor and extensor muscles of the left and right forearm.

ACCs and EMGs were band-pass filtered to avoid aliasing effects and undesired slow drifts (ACC: 0.5 Hz – 50 Hz, EMG: 80 Hz–500 Hz). All data were simultaneously sampled at 1000 Hz and stored on computer using a special software (37). The mean was subtracted from each time series. Finally, the series were tapered with a Bartlett-Window to reduce spectral leakage (8) and normalized to unit variance. In addition, EMGs were digitally full wave rectified for spectral and cross-spectral analysis (33; 20). The rectification yields a time series which reflects the muscle activity that is encoded in the envelope of the originally measured signal.

EEG recordings were performed using a 64-channel EEG system. The potential field measured over the scalp was transformed into the reference free current density distribution which reflects the underlying cortical activity by calculating second spatial derivatives (29; 30).

2.2 Cross-Spectral Analysis

The power spectrum $S_x(\omega)$ of a zero mean process $X(t)$ is defined as the Fourier transform of the auto-covariance function $\mathrm{ACF}(t') = \langle X(t)\, X(t-t')\rangle$:

$$S_x(\omega) = \frac{1}{2\pi} \sum_t \mathrm{ACF}(t) \exp(-i\,\omega\, t)\,, \quad \omega \in (-\pi, \pi]\,, \tag{1}$$

where $\langle \cdot \rangle$ denotes expectation (8). The estimation of the power spectrum is performed by a direct spectral estimation (8; 47; 2), based on the Fourier transform $\mathrm{FT}_x(\omega)$ of the measured data $x(t)$

$$\mathrm{FT}_x(\omega_k) = \frac{1}{\sqrt{N}} \sum_{t=1}^{N} x(t) \exp(-i\,\omega_k\, t)\,, \quad k = \frac{-N+1}{2}, \ldots, \frac{N}{2}. \tag{2}$$

The periodogram $\mathrm{Per}_x(\omega_k)$ is defined as the squared modulus of $\mathrm{FT}_x(\omega_k)$. Whenever the auto-covariance function $\mathrm{ACF}(t)$ is decaying fast enough for larger lags, the Fourier transform $\mathrm{FT}_x(\omega_k)$ is asymptotically Gaussian distributed with variance given by $S_x(\omega)$. Therefore, the periodogram $\mathrm{Per}_x(\omega_k)$ is distributed as χ^2_2, a random variable which does not represent a consistent estimator for the spectrum because its variance is equal to its mean. Note, that this holds for deterministic chaotic as well as for (nonlinear) stochastic processes as long the auto-covariance function $\mathrm{ACF}(t)$ is decaying sufficiently fast. To obtain a consistent estimator of the spectrum, the periodogram has to be smoothed by a window function W_j

$$\widehat{S_x}(\omega_k) = \frac{1}{2\pi} \sum_{j=-h}^{h} W_j \,\mathrm{Per}_x(\omega_{k+j}) \quad , \tag{3}$$

The simplest example for the weight function W_j is an equal weighted "square" window, the so called Daniell estimator. We choose a triangular window (i.e. a Bartlett estimator) with an adaptive, frequency dependent width (58) for the auto-spectral estimations.

Similar to the univariate case, the cross-spectrum $\mathrm{CS}(\omega)$ of two zero-mean processes $X(t)$ and $Y(t)$ is defined as the Fourier transform (FT) of the cross-correlation function $\mathrm{CCF}(t') = \langle X(t)\, Y(t-t')\rangle$. Again, the estimation is based on smoothing of the cross-periodogram. The coherence spectrum $\mathrm{Coh}(\omega)$ is given by the modulus of the cross-spectrum $\mathrm{CS}(\omega)$ normalized by the respective auto-spectra $S_x(\omega)$ and $S_y(\omega)$ (8; 47; 4; 62)

$$\mathrm{Coh}(\omega) = \frac{|\mathrm{CS}(\omega)|}{\sqrt{S_x(\omega) S_y(\omega)}} \quad . \tag{4}$$

The phase spectrum $\Phi(\omega)$ is defined by

$$\mathrm{CS}(\omega) = |\mathrm{CS}(\omega)| \, \exp(i\,\Phi(\omega)) \quad . \tag{5}$$

The coherence and phase spectra were estimated by replacing the cross- and auto-spectra in Eq. (4) by their respective estimated quantities.

The coherence can be interpreted as a measure of linear predictability (8; 47) — it equals one whenever $X(t)$ is obtained from $Y(t)$ by a linear operator $L(.)$. It is important to note, that the interpretation of the coherence does not rely on the linearity of the processes $X(t)$ and $Y(t)$. The only condition $Y(t)$ has to fulfill is that the spectrum must be broad band. It can e.g. also be chaotic or nonstationary. Besides the simple case where $Y(t)$ and $X(t)$ are indeed uncorrelated, at least the following reasons can result in a coherence unequal one:

- A nonlinear relationship between $X(t)$ and $Y(t)$
- Additional influences on $X(t)$ apart from $Y(t)$
- Estimation bias due to misalignment (26)
- Observational noise

With respect to a possible nonlinear relationship between $X(t)$ and $Y(t)$ it should be mentioned that the coherence is equal to zero if the relationship between the processes is a quadratic one. If it is a cubic one, the coherence will still be able to detect the relation since a linear approximation will explain a part of the variance. In our applications the observational noise turned out to be the most prominent reason for observing a reduced coherence. If $Y(t)$ is a linear function of $X(t)$ but the measurements of $Y(t)$ and $X(t)$ are covered by white observational noise of variance σ_y^2 and σ_x^2, the resulting coherency is given by (62):

$$\mathrm{Coh}(\omega) = \sqrt{1 - \frac{\sigma_x^2 S_y + S_x \sigma_y^2 + \sigma_x^2 \sigma_y^2}{(S_x + \sigma_x^2)(S_y + \sigma_y^2)}} \quad , \tag{6}$$

where the argument ω was suppressed on the right hand for ease of notation and σ_x^2 and σ_y^2 denote the constant power spectra of the observational noise. Thus, the coherency is a function of the frequency dependent signal to noise ratio.

The interpretation of the phase spectrum is more difficult. For the following cases the phase spectrum can be calculated analytically :

- If the process $X(t)$ is a time delayed version of process $Y(t)$, i.e. $X(t) = Y(t - \Delta t)$, the phase spectrum is given by a straight line with its slope determined by Δt :

$$\Phi(\omega) = \Delta t \, \omega \quad . \tag{7}$$

- If $X(t)$ is the derivative of $Y(t)$, i.e. $X(t) = \dot{Y}(t)$ a constant phase spectrum of $-\frac{\pi}{2}$ results.

$$\Phi(\omega) = -\pi/2 \quad . \tag{8}$$

- In the case of a linear autoregressive (AR) process of order 2 (AR[2]):

$$X(t) = a_1 X(t-1) + a_2 X(t-2) + \epsilon(t), \quad \epsilon(t) \sim \mathrm{N}(0, \sigma^2) \tag{9}$$

the phase spectrum between the driving noise $\epsilon(t)$ and the resulting process is given by :

$$\Phi(\omega) = \arctan\left(\frac{a_1 \sin\omega + a_2 \sin 2\omega}{1 - a_1 \cos\omega - a_2 \cos 2\omega}\right) \quad . \tag{10}$$

Since an AR[2] process represents a stochastically driven damped linear oscillator, Eq. (10) is the discrete time version of the well-known sigmoidal behavior of the phase spectrum for the corresponding time-continuous resonant system. This relation is discussed in detail in (62). Note, that the parameters of an AR[2] process can be related to the period T and the relaxation time τ of the damped oscillator by:

$$\begin{aligned} a_1 &= 2\cos(2\pi/T)\exp(-1/\tau) \qquad (11) \\ a_2 &= -\exp(-2/\tau) \qquad . \qquad (12) \end{aligned}$$

If one of the theoretical functional behaviors of the phase spectrum is observed in measured data, it may allow for an identification of the system.

For the application to measured data, the first question is if there is a significant coherence. The critical value s for the null hypothesis of zero coherence for a significance level α is given by (8) :

$$s = \sqrt{1 - \alpha^{\frac{2}{\nu-2}}} \quad , \qquad (13)$$

where ν is the so called equivalent number of degrees of freedom, determined by the window function $W(j)$ used and the tapering (2; 4). Confidence intervals for the coherence are given in (2). The variance of the estimator for the phase spectrum $\widehat{\Phi}(\omega)$ depends on the coherence (47):

$$var(\widehat{\Phi}(\omega)) = \frac{1}{\nu}\left(\frac{1}{Coh^2(\omega)} - 1\right) \quad . \qquad (14)$$

Eq. 14 holds if the coherence is significantly larger than zero. For a coherence towards zero, the distribution of the estimated phase approaches the uniform distribution in $[-\pi, \pi]$. Therefore, the phase spectrum cannot be estimated reliably in the case of small coherence. This poses an important limitation for the applicability of the phase spectrum to infer the functional form of the relationship between the processes. If the confidence regions of the phase spectrum are small only in a narrow frequency band it is not possible to decide whether e.g. Eq. (7) or Eq. (10) is the true underlying phase spectrum.

It is important to note that the statistical properties of the coherence and phase spectrum are known and easily calculated. This does not hold for the statistical properties of the estimated cross-correlation function. Here, the estimation errors are, in general, not independent for different lags. These correlations may lead to effects that are in the same order as the true cross-correlations. Therefore, the cross-correlation function can not be used to gain information about the relation between the processes (62). Note, that this situation carries over to more general non-linear measures of dependence as the trans information (63) or phase synchronization (54).

2.3 Analyzing Multivariate Time Series

In extending cross-spectral analysis to the multivariate case, one faces a problem which is common to all methods that are designed to analyze bivariate data when applied to multivariate data: If a bivariate method detects a relation between two signals, it can not be decided if there is an underlying direct or indirect connection. The correlation between the number of babies and the numbers of storks in industrial developed countries serves as a popular example.

To detect spurious correlations and identify true relations in multivariate data sets, the notion of conditional independence has been introduced in the frame of graphical models (66; 38; 12). If a bivariate subset of data is independent when the information of the remaining data is taken into account the two variables are called conditionally independent. For linear regression this leads to the notion of partial correlation. These procedures have been generalized to point processes and time series (6; 49; 25; 5; 14; 13). Instead of the cross-spectrum introduced in Sec. 2.2 one considers the partial cross-spectrum. The partial cross-spectrum $\mathrm{PCS}_{X_1 X_2|Y}(\omega)$ between the processes X_1 and X_2 given the information of the remaining processes denoted by Y can be calculated by (4):

$$\mathrm{PCS}_{X_1 X_2|Y}(\omega) = \mathrm{CS}_{X_1 X_2}(\omega) - \mathrm{CS}_{X_1 Y}(\omega) S_Y(\omega)^{-1} \mathrm{CS}_{Y X_2}(\omega) \qquad (15)$$

Based on the partial cross-spectrum partial coherence and partial phase spectra are obtained analogously to Eqs. (4,5). The critical value s for the null hypothesis of zero partial coherence depends on the dimension L of the partialized processes Y. For a significance level α, in generalization of Eq. (13) it is given by (25):

$$s = \sqrt{1 - \alpha^{\frac{2}{\nu - 2L - 2}}} \quad . \qquad (16)$$

The variance of the partial phase spectrum is by given Eq. (14), applying the partial coherence instead of the conventional coherence.

The notion of “graphical model” for this kind of analysis is due to the fact that the consideration of all the significant pairwise partial coherences for a multivariate time series leads to a graph where the edges in the graph represent direct coupling between the corresponding components of the time series (14; 13).

3 Applications

In this section we give various applications for cross-spectral analysis of tremor time-series.

3.1 The Contribution of Reflexes to Physiological Tremor

The physiological tremor of healthy subjects can be subclassified with respect to the presence of spectral peaks in the EMG time series. Fig. 2 gives an example for ACC and EMG data for a typical physiological hand tremor where the EMG does not exhibit peaks. The left column of Fig. 3 shows the spectrum, coherence and phase spectra for a the data shown in Fig. 2. The single broad peak of the ACC spectrum suggests a linear second order process for the data (24; 55):

Fig. 2 around here

$$EMG(t) = \eta(t) \tag{17}$$

$$x(t) = a_1 x(t-1) + a_2 x(t-2) + EMG(t) \tag{18}$$

$$ACC(t) = \ddot{x}(t) \tag{19}$$

where $\eta(t)$ denotes white noise and $x(t)$ the position of the hand. It should be noted that the measured data contain white additive observational noise. The parameter a_1 and a_2 are related to the resonant frequency of the hand and the damping of the process due to the muscles and tissue by Eqs. (11,12). Since the model is linear the parameter can be fitted from the data. The right column of Fig. 3 shows the results for a realization of the fitted model analogous to the left column of Fig. 3 for the measured data. Confidence regions of the auto- and coherence spectra are not given for ease of clarity. The only statistically significant differences in the results appear for low frequencies. Here the coherence for the data of the model is larger than for the measured data and, consequently, the errors of the phase spectrum are larger. The reason for this is the so-called cardio-ballistic effect (22). The heart beat excites the hand at a frequency around 1 Hz. Since this additional influence is not captured by our model, the model overestimates the coherence. Apart from that the phase spectrum of the data and the model show the expected sigmoidal behavior of a resonant oscillator, Eq. (10), with the characteristic jump at the resonant frequency. The fact that the phase spectrum values ranges from $-\pi$ to 0 and not as could have been expected from 0 to π is explained by the circumstance that the acceleration, not the position of the hand is measured, see Eq. (8). In terms of physics and physiology the result shows that this kind of tremor represents a resonant oscillation of the hand that is driven by uncorrelated firing motoneurons and that the measured EMG represents a Newtonian force by which the muscle acts on the hand (62). Comparable results were obtained for 58 subjects with physiological tremor and a flat EMG spectrum.

In the case of peaks in the EMG spectra there are two possible reasons. First, there can be an oscillator in the central nervous system that drives the hand. Second, reflex loops can serve for a oscillatory EMG activity. To capture both possible effects we use the following model:

$$\begin{aligned} c(t) &= b_1 c(t-1) + b_2 c(t-2) + \epsilon(t) & (20) \\ r(t) &= \alpha\, f(x(t-\delta t)) & (21) \\ EMG(t) &= c(t) + r(t) + \eta(t) & (22) \\ x(t) &= a_1 x(t-1) + a_2 x(t-2) + EMG(t) & (23) \\ ACC(t) &= \ddot{x}(t) & (24) \end{aligned}$$

where $c(t)$ denotes the central input, $r(t)$ the reflex contribution and $f(.)$ the nonlinearity of the reflex modeled by the tangens hyperbolicus. The central input is described by an AR[2] process. This model presents a nonlinear, stochastic, inhomogeneous delay differential equation (61). To test for the contribution of the reflex in this model, it would be necessary to test whether the coefficient α is consistent with zero. Unfortunately, no techniques are known to the authors to estimate parameters of the above equations from noisy data.

In order to identify the role of reflexes in the generation of physiological tremor, we investigated in model simulations phase spectra and auto-spectra under the two hypothesis that 1) reflexes contribute significantly ($\alpha \neq 0$) and 2) that they do not play a significant role ($\alpha = 0$) (61).

For the non-reflex case the phase spectrum can be calculated analytically

(62). The shape of the phase spectrum only depends on the properties of the mechanical, resonant oscillator and is independent of the driving force. In the reflex case the feedback does not modify the phase spectrum. But the apparent resonance frequency in the auto-spectrum of the mechanical oscillator (i.e. the ACC in case of tremor time series) moves depending on the chosen feedback delay. Thus, a significant difference between the resonance frequency in the phase spectrum and the peak frequency in the auto-spectrum points to a significant contribution of reflexes in physiological tremor (61).

To identify the contribution of reflexes in tremor data the following steps were performed. First, the peak frequency in the auto-spectrum of the ACC was estimated. Confidence intervals are given by a bootstrap procedure described in detail in (59; 60). Secondly, the resonance frequency in the phase spectrum was estimated by fitting Eq. (10) to the estimated phase spectrum. Since the confidence regions for the estimated phase spectrum are available, a confidence region for the resonance frequency can be obtained. Fig. 4 gives an example in which to two respective frequency estimates are statistically different. An example where no reflex could be detected is given in (61). In 35 time series recorded from 19 subjects with the respective type of physiological tremor, we clearly found that reflexes contribute to the tremor (61).

Fig.4 around here

In simulation studies based on Eqs. (20-24) using a delay time of 35 ms corresponding to a possible segmental stretch reflex, we found a shift of the ACC peak frequency to higher values. For longer delay times corresponding to central loops, we found shifts to lower frequencies (61). In the measured time series, in the majority of cases we observed shifts to lower frequencies. This indicates that more complex structures than the segmental stretch reflex are involved in the process, perhaps a combination of different reflex loops.

However, there is no evidence in the data that reflex loops primarily cause the tremor. They alter the frequency, relaxation time and amplitude of existing oscillations in a limited range. The primary cause of this type of physiological tremor is the resonant behavior of the hand and a synchronized EMG activity that is generated centrally. Evidence for the central component is given in the following section.

3.2 Physiological Tremor and Mirror-Movements

Apart from the resonant component, a component around 8-12 Hz is often present in physiological tremor (21). While the frequency of the resonant component can be altered by loading following the $\omega_{peak} \propto \sqrt{1/m}$ law for a resonance frequency, the 8-12 Hz component does not change under loading. This has lead to the hypothesis that this component is generated centrally. To reveal whether the motor cortex is involved in this process we compared coherences of EMG time series recorded from the right and the left hand of subjects with the motor abnormality of persistent mirror movement to those of control subjects. Neurophysiological studies have shown that mirror movements are caused by abnormal transmitting pathways that project from the motor cortex to both sides of the body (11; 28). In normal subjects the projections are only to the contralateral side. Assuming a central mechanism or driving force that involves the motor cortex in the generation of physiological tremor, EMG activity should be coherent between the right and left side of the body for the subjects with mirror movements.

Fig. 5 displays the results for three subjects with mirror movements and healthy controls. All subjects with mirror movements exhibit a significant coherence (36; 34). In contrast, controls do not show a coherent activity. These results suggest the presence of bilateral and independent central generators of the 8-12 Hz component in physiological tremor and completes the results of the first application discussed in Sec. 3.1. Fig. 5 around here

3.3 Side-to-Side Coherence of Muscle Activity in Pathological Tremors

In this section we address the question if the different pathological tremors are side-to-side coherent, similar as discussed in Sec. 3.2 for physiological tremor.

Seven patients with orthostatic tremor, 76 essential tremors and 70 Parkinsonian tremors were investigated. The results show a clear-cut difference between Parkinsonian and essential tremor on the one hand and the orthostatic tremor on the other hand. All investigated orthostatic tremor patients exhibited a significant side-to-side coherence with surprisingly high values (up to 0.98), while only as many as statistically expected essential and Parkinsonian patients showed a significant coherence, despite corresponding tremor amplitudes and similar signal-to-noise ratios in orthostatic tremor and Parkinsonian, respectively essential tremor. This points to a single central oscillator generating orthostatic tremor, while different oscillators are responsible for the tremor of different limbs in essential and Parkinsonian tremor (36; 48).

It is still under discussion whether orthostatic tremor is a variant within the spectrum of essential tremor or a separate entity (65; 10; 44; 7). Our results clearly separate orthostatic tremor and essential tremor as different forms of tremor. Furthermore, this method could serve as an objective and low-cost tool for the diagnosis of orthostatic tremor.

3.4 EEG and EMG coherence

Parkinsonian tremor is thought to be generated by central nervous structures. Using the magnetoencephalogram, it has been shown that cerebral cortex is involved (64; 54). In this study we investigated whether cortical activity related to Parkinsonian tremor can be detected by EEG (27). Similar approaches were unsuccessful in the past (32; 51).

Five patients with unilateral Parkinsonian tremor were included in this study. In all patients we a found highly significant coherence between the EEG and EMG time series at the tremor frequency and its higher harmonics. Fig. 6 displays isocoherence maps for the tremor frequency over the scalp of the five subjects. In all cases the maximum coherence was located over the cortical motor area of the contralateral side of the tremor affected hand. For the patients whose results are displayed in Fig. 6e and f the coherence was highest for the frequency of the first harmonics which is located at twice the tremor frequency. This can be explained by the fact that the cortical areas in

Fig. 6 around here

the motor cortex that drive the extensor and the flexor muscles of the hand are only a few millimeter apart which leads to a superposition of their signals at the EEG electrodes. Since these patients exhibit an alternating activation of flexor and extensor muscles this results in a component of the EEG signal with twice the frequency of the tremor oscillation. This component is coherent with the first harmonics of the EMG signal. This result is consistent with the finding by Tass et al. (54) who reported a $2:1$ synchronization between MEG and EMG.

Of special importance is the result displayed in Fig. 6c. Here, a high coherence to the EMG is also found at electrode P4 which represents the sensomotor cortex. Furthermore, there is a significant coherence between the electrodes P4 and C2a which is located above the motor cortex. There are two different possible explanations for this finding. First, all observed coherences correspond to true relations between the investigated processes, i.e. there is a closed signal transmission loop. Second, the coherence between the sensomotor and the motor cortex is spurious, meaning that there is no underlying direct connection but that the coherence is caused only by propriorezeptive afferences. It is a fundamental limitation of methods designed to analyze bivariate processes when applied to multivariate processes that these alternatives can not be decided. We calculated the partial coherence introduced in Sec. 2.3 between the two EEG channels given the information of the EMG. The partial coherence is smaller than the coherence between the two channels but does not fall below the level of significance. Thus, unfortunately, no conclusive conclusion can be drawn in this case.

In another experiment, we measured EEG and left hand extensor-EMG in a healthy subject during an externally enforced oscillation of the hand with 1.9 Hz. Fig. 7 shows the resulting isocoherence maps between left hand extensor-EMG and EEG at the frequency of the oscillation. A significant coherence is found for the channels P1 and C2P. These results were reproduced in nine repetitions of the experiment.

Fig. 7 around here

Fig. 8 displays the spectra of the time series on the diagonal, the conventional and the partial coherence spectra between the respective time series on the subdiagonal. The nonlinearity of the processes is apparent from the higher harmonics in the spectra.

The confidence levels for zero coherence and zero partial coherence, differ due to the dimension L of the partialized processes Y, see Eqs. (13,16). For the results displayed in Fig. 8 this dimension is one. Therefore, the two confidence levels are virtually the same and we plotted only those for zero partial coherence (at the 5% level). They are conservative bounds for the conventional coherence. Moreover, we chose simultaneous confidence levels. This solves the problem of multiple testing in a statistically conservative way (50). This procedure ensures that every time the level is exceeded represents a significant coherence at the nominal level of significance. A significant coherence is found at the tremor frequency and its higher harmonic between all three channels. The partial coherence between the left hand extensor-EMG and the EEG channel P1 falls below the level of significance. This suggests that the coherence between P1 and the EMG signal does not represent a direct connection, but that the signal transfer is mediated via C2P.

4 Discussion

We discussed bivariate cross-spectral analysis and its generalization to the multivariate case in the frame of graphical models and present numerous applications to tremor data. Although cross-spectral analysis initially was developed in the frame of linear stochastic processes its applicability is not limited to this class of processes. It may allow for insights also for nonlinear processes as long as the relation between the processes is linear. We demonstrated this for time series of pathological tremors that represent nonlinear processes (24; 56; 57). For example, the high coherence between left and right sided tremor time series in orthostatic tremor led to the conclusion of a single oscillator driving this tremor in all muscles of the body, whereas in Parkinsonian and essential tremor different oscillators for different limbs must be hypothesized. Some physiological tremors exhibit a reflex contribution. Formally, such systems have to be described by a non-linear, stochastic, inhomogeneous delay differential equation. Even for this system (linear) cross-spectral analysis could successfully be applied by means of testing for the presence of the reflex contribution. Here, we took advantage of the fact that in absence of the reflex loop the system is well described by a second order linear stochastic process reflecting the resonant nature of this tremor.

Stationarity is a crucial issue for the applicability of many time series analysis methods and tremor is not a stationary process in a strict mathematical sence. However, for cross-spectral analysis it is not required that the involved processes are stationary but only that the relation between the processes is time independent. For the tremor processes under investigation this relation is determined by quantities like the mass of the hand and the stiffness of muscles and tissue for the investigations in Section 3.1 and neural connectivity in Sections 3.2-3.4. This quantities can be considered as constant for the 30 seconds of measurement. Moreover, analyses reported in (55) and (57) show that physiological, essential and parkinsonian tremor time series are consistent with stationary second order stochastic processes, linear in the first case, nonlinear in the two latter cases. This consistency does not prove stationarity but claims that these processes are statistically indistiguishable from stationary processes.

Apart from the insights in the mechanisms underlying the different forms of tremor, cross-spectral methods might be helpful in a daily clinical routine as a diagnostic tool, e.g. for discriminating orthostatic from essential tremor.

The successful applications of cross-spectral analysis to the measured time series rely heavily on the fact that the statistical properties of the estimates are known which is, unfortunately, not the case for many methods from nonlinear dynamics to investigate corresponding relations.

Whenever it comes to analyze multivariate time series by means of methods that were developed to analyze bivariate data, the problem occurs that it is not possible to decide by these methods whether a significant relation between two time series corresponds to a direct coupling or is only a result of an indirect connection. Cross-spectral analysis can be generalized to deal with this problem in the frame of graphical models. Therefore, partial cross-spectra are estimated in which the relation between two time series is investigated taking the information of the remaining data into account. For simultaneous measurements of EEG and enforced tremor activity, we showed that this method may reveal cortical transmission pathways.

Acknowledgments

This work was supported by the German Federal Ministry of Education, Science, Research and Technology (BMBF) by the grant "Verbundprojekte in der Mathematik" (ML).

References

[1] J. H. J. Allum. Segmental reflex, muscle mechanical and central mechanisms underlying human physiological tremor. In L.J. Findley and R. Capildeo, editors, *Movement Disorders: Tremor*, pages 135–155. Macmillan, London, 1984.

[2] P. Bloomfield. *Fourier Analysis of Time Series: An Introduction.* John Wiley & Sons, New York, 1976.

[3] A. Boose, S. Spieker, C.H. Jentgens, and J. Dichgans. Wrist Tremor: Investigation of Agonist-Antagonist Interaction by means of Long-term EMG Recording and Cross-Spectral Analysis. *Electroencephalogr. Clin. Neurophysiol.*, 101:355–363, 1996.

[4] D. R. Brillinger. *Time Series: Data Analysis and Theory.* Holden-Day, Inc., San Francisco, 1981.

[5] D.R. Brillinger. Remarks concerning graphical models for time series and point processes. *Revista de Econometrica*, 16:1–23, 1996.

[6] D.R. Brillinger, H.L. Bryant, and J.P. Segundo. Identification of synapthic interactions. *Biological Cybernetics*, 22:213–228, 1976.

[7] T.C. Britton, P. D. Thompson, W. van der Kamp, J. C. Rothwell, B. L. Day, L. J. Findley, and C. D. Marsden. Primary orthostatic tremor: Further observations in six cases. *J. Neurol.*, 239:209–17, 1992.

[8] P.J. Brockwell and R.A. Davis. *Time Series: Theory and Methods*. Springer, New York, 1991.

[9] C.N. Christakos. A linear Stochastic Model for Single Motor Units. *Biological Cybernetics*, 44:79–89, 1982.

[10] L Cleeves, J Cowen, and L J Findley. Orthostatic tremor: diagnostic entity or variant of essential tremor. *J. Neurol. Neurosurg. Psych.*, 52:130–31, 1987.

[11] L.G. Cohen, J. Meer, I. Tarkka, S. Bierner, D.B. Leiderman, R.M. Dubinsky, J.N. Sanes, B. Jabbari, B. Branscum, and M. Hallett. Congenital Mirror Movements. *Brain*, 114:381–403, 1991.

[12] D.R. Cox and N. Wermuth. *Multivariate Dependencies*. Chapman and Hall, London, 1996.

[13] R. Dahlhaus. Graphical interaction models for multivariate time series. *Metrika*, 1999, submitted.

[14] R. Dahlhaus, M. Eichler, and J. Sandkühler. Identification of synaptic connections in neural ensembles by graphical models. *J. Neuroscience Methods*, 77:93–107, 1997.

[15] G. Deuschl, P. Bain, and M. Brin. Consensus statement of the Movement Disorder Society on tremor. *Mov. Disorder*, 13:2–23, 1998.

[16] G. Deuschl, H Blumberg, and C. H. Lücking. Tremor in Reflex Sympathetic Dystrophy. *Arch. Neurol.*, 48:1247–1252, 1991.

[17] G. Deuschl, P. Krack, M. Lauk, and J. Timmer. Clinical neurophysiology of tremor. *J. Clinic. Neurophys.*, 13:110–121, 1996.

[18] R. Elble. Central mechanisms of tremor. *J. Clin. Neurophysiol.*, 13:133–44, 1996.

[19] R. J. Elble. Physiologic and essential tremor. *Neurology*, 36:225–31, 1986.

[20] R.J. Elble and W.C. Koller. *Tremor.* John Hopkins University Press, Baltimore, 1990.

[21] R.J. Elble and J.E. Randall. Motor-Unit Activity Responsible for 8- to 12-Hz Component of Human Physiological Finger Tremor. *J. Neurophysiol.*, 39:370–83, 1976.

[22] R.J. Elble and J.E. Randall. Mechanistic Components of Normal Hand Tremor. *Electroenceph. clin. Neurophys.*, 44:72, 1978.

[23] J.R. Fox and J.E Randall. Relationship between Forearm Tremor and the Biceps Electromyogram. *J. Appl. Physiol.*, 29:103–8, 1970.

[24] C. Gantert, J. Honerkamp, and J. Timmer. Analyzing the dynamics of tremor time series. *Biol. Cybern.*, 66:479–484, 1992.

[25] D.M. Halliday, J.R. Rosenberg, A.M. Amjad, P. Breeze, B.A. Conway, and S.F. Farmer. A framework for the analysis of mixed time series/point process data – Theory and application to the study of physiological

tremor, single motor unit discharges and electromyograms. *Prog. Biophys. molec. Biol.*, 64:237–278, 1995.

[26] E.J. Hannan and P.J. Thomson. The estimation of coherency and group delay. *Biometrika*, 58:469–481, 1971.

[27] B. Hellwig, S. Haussler, M. Lauk, B. Köster, B. Guschlbauer, R. Kristeva-Feige, J. Timmer, and C.H. Lücking. Electroencephalography reveals tremor-correlated cortical activity in patients with Parkinson's disease. *Electroencephalogr. Clin. Neurophysiol., submitted*, 1999.

[28] J. Hermsdörfer, A. Danek, T. Winter, C. Marquardt, and N. Mai. Persistent Mirror Movements: Force and Timing of "Mirroring" are Task–ependent. *Experimental Brain Research*, 104:126–134, 1995.

[29] B. Hjorth. An on-line transformation of EEG scalp potentials into orthogonal source derivations. *Electroencephalogr. Clin. Neurophysiol.*, 39:526–530, 1975.

[30] B. Hjorth. Principals for transformation of scalp EEG from potential field into source distribution. *J. Clin. Neurophysiol.*, 8:391–396, 1991.

[31] P.A. Iaizzo and R.S. Pozos. Analysis of Multiple EMG and Acceleration Signals of Various Record Lengths as a means to study Pathological and Physiological Oscillations. *Electromyogr. Clin. Neurophysiol.*, 32:359–67, 1992.

[32] H.H. Jaspar and H.L. Andrews. Brain potentials and voluntary muscle activity in man. *J. Neurophys.*, 1:87–100, 1938.

[33] H.L. Journée. Demodulation of amplitude modulated noise: A mathematical evaluation of a demodulator for pathological tremor EMG's. *IEEE Trans. Biomed. Eng.*, 30:304–8, 1983.

[34] B. Köster, M. Lauk, J. Timmer, B. Guschlbauer, T. Winter, F.X. Glocker, G. Deuschl, and C.H. Lücking. Central mechanisms in enhanced physiological tremor. *Neuroscience Letters*, 241:135–138, 1998.

[35] B. Köster, M. Lauk, J. Timmer, M. Poersch, B. Guschlbauer, F.X. Glocker, G. Deuschl, and C.H. Lücking. Involvement of cranial muscles and high intermuscular coherence in orthostatic tremor. *Annales Neurology*, 45:384–388, 1999.

[36] M. Lauk, B. Köster, J. Timmer, G. Guschlbauer, G. Deuschl, and C.H. Lücking. Side-to-side correlation of muscle activity in physiological and pathological human tremors. *Electroenceph. clinical Neurophys.*, 110:1774–1783, 1999.

[37] M. Lauk, J. Timmer, C.H. Lücking, J. Honerkamp, and G. Deuschl. A software for recording and analysis of tremor. *Computer Methods and Programs in Biomedicine*, 60:65–77, 1999.

[38] S.L. Lauritzen. *Introduction to Graphical Modelling.* Springer, New York, 1996.

[39] F.A. Lenz, H.C. Kwan, R.L. Martin, R.R. Tasker, J.O. Dostrovsky, and Y.E. Lenz. Single unit analysis of the human ventral thalamic nuclear

group: Tremor related activity in functionally identified cells. *Brain*, 117:531–43, 1994.

[40] F.A. Lenz, R.R. Tasker, H.C. Kwan, S. Schnider, R. Kwong, Y. Murayama, J.O. Dostrovsky, and J.T. Murphy. Single unit analysis of the human ventral thalamic nuclear group: Correlation of thalamic "tremor cells" with the 3–6 Hz component of parkinsonian tremor. *J. Neurosci.*, 8:754–64, 1988.

[41] O.C.J. Lippold. Oscillation in the Stretch Reflex Arc and the Origin of the Rhythmical, 8–12 Hz Component of Physiological Tremor. *Journal of Physiology*, 206:359–82, 1970.

[42] R. Llinás and D. Paré. Role of Intrinsic Neuronal Oscillations and Network Ensembles in the Genesis of Normal and Pathological Tremor. In L.J. Findley and W.C. Koller, editors, *Handbook of Tremor Disorders*, chapter 2, page 7. Marcel Dekker, New York, 1995.

[43] C.-H. Lücking, B. Köster, B. Guschlbauer, M. Lauk, and J. Timmer. Parkinsonian and essential tremor: Different entities or different manifestations of the same disorder. *Advances in Neurology*, 80:335–339, 1999.

[44] S.M. Papa and A.S. Gershanik. Orthostatic tremor: an essential tremor variant. *Mov. Disord.*, 3:97–108, 1988.

[45] S.M. Pashda and R.B. Stein. The Base of Tremor during Maintained Posture. In R B Stein, K G Pearson, R S Smith, and J B Redford,

editors, *Control of Posture and Locomotation*, pages 415–19. Plenum Press, New York, 1973.

[46] R.S. Pozos and P.A. Iaizzo. Shivering and Pathological and Physiological Clonic Oscillations of the Human Ankle. *J. Appl. Physiol.*, 71:1929–32, 1991.

[47] M.B. Priestley. *Spectral analysis and time series.* Academic Press, London, 1989.

[48] J. Raethjen, M. Lindemann, H. Schmajohann, R. Wenzelburger, G. Pfister, and Deuschl G. Multiple oscillators are causing Parkinson and essential tremor. *Movement Disorder, submitted*, 1999.

[49] J.R. Rosenberg, A.M. Amjad, P. Breeze, D.R. Brillinger, and D.M. Halliday. The Fourier appraoch to the identification of functional coupling between neuronal spike trains. *Prog. Biophys. molec. Biol.*, 53:1–31, 1989.

[50] L. Sachs. *Applied Statistics.* Springer, New York, 1984.

[51] R.S: Schwab and S. Cobb. Simultaneous electromyograms and electroencephalograms in paralysis agitans. *J. Neurophys.*, 2:36–41, 1939.

[52] R.N. Stiles. Mechanical and neural feedback factors in postural hand tremors of normal subjects. *J. Neurophys.*, 44:40–59, 1980.

[53] R.N. Stiles. Lightly Damped Hand Oscillations: Acceleration–Related Feedback and System Damping. *J. Neurophysiol.*, 50:327–43, 1983.

[54] P. Tass, M.G. Rosenblum, J. Weule, J. Kurths, A. Pikovsky, J. Volkmann, A. Schnitzler, and H.J. Freund. Detection of $n:m$ phase locking from noisy data: application to magnetoencephalography. *Phys. Rev. Lett.*, 81:3291–3295, 1998.

[55] J. Timmer. Modeling noisy time series: Physiological tremor. *Int. J. Bif. Chaos*, 8:1505–1516, 1998.

[56] J. Timmer, C. Gantert, G. Deuschl, and J. Honerkamp. Characteristics of hand tremor time series. *Biol. Cybern.*, 70:75–80, 1993.

[57] J. Timmer, S. Häußler, M. Lauk, and C.H. Lücking. Pathological tremors: Deterministic chaos or nonlinear stochastic oscillators ? *CHAOS, submitted*, 1999.

[58] J. Timmer, M. Lauk, and G. Deuschl. Quantitative analysis of tremor. *Electroenceph. clin. Neurophys.*, 101:461–468, 1996.

[59] J. Timmer, M. Lauk, and C.H. Lücking. Confidence regions for spectral peak frequencies. *Biometrical Journal*, 39:849–861, 1997.

[60] J. Timmer, M. Lauk, and C.H. Lücking. A test for a difference between spectral peak frequencies. *Computational Statistics and Data Analysis*, 30:45–55, 1999.

[61] J. Timmer, M. Lauk, W. Pfleger, and G. Deuschl. Cross-spectral analysis of physiological tremor and muscle activity. II. Application to synchronized EMG. *Biol. Cybern.*, 78:359–368, 1998.

[62] J. Timmer, M. Lauk, W. Pfleger, and G. Deuschl. Cross-spectral analysis of physiological tremor and muscle activity. I. Theory and application to unsynchronized EMG. *Biol. Cybern.*, 78:349–357, 1998.

[63] J.A. Vastano and H.L. Swinney. Information transport in spatio temporal systems. *Phys. Rev. Lett.*, 60:1773–1776, 1988.

[64] J. Volkmann, M. Joliot, A. Mogilner, A.A. Ioannides, F. Lado, E. Fazzini, U. Ribary, and R. Llinás. Central motor loop oscillations in parkinsonian resting tremor revealed by magnetoencephalography. *Neurology*, 46:1359–70, 1996.

[65] A.S. Wee, S.H. Subramony, and R.D. Currier. Orthostatic tremor in familial essential tremor. *Neurology*, 36:1241–5, 1986.

[66] J. Whittaker. *Graphical Models in Applied Multivariate Statistics*. John Wiley, Chichester, 1995.

[67] R.R. Young and K.E. Hagbarth. Physiological Tremor Enhanced by Manoeuvres affecting the Segmental Stretch Reflex. *Journal of Physiology*, 43:248–56, 1980.

Figure captions

Fig. 1 Examples for the recorded data. (a) Accelerometer, (b) raw EMG and (c) EEG for a patient suffering from Parkinson's Disease.

Fig. 2 Acceleration of the hand (a) and rectified EMG (b) of physiological tremor.

Fig. 3 Results for a physiological tremor. (a): power spectra (EMG: dashed line in units of $(\mu V)^2$, ACC: solid line, in units of $(mm/sec^2)^2$), (b): coherence spectrum, the straight line represents the 5% significance level for the hypothesis of zero coherence, (c): phase spectrum with 95% confidence intervals. Confidence intervals for the power spectra and the coherence are not displayed for reasons of clarity. (d)-(f) display the results for a linear model fitted to the data.

Fig. 4 Analysis of an enhanced physiological tremor. a: power spectra (EMG: dashed line in units of $(\mu V)^2$, ACC: solid line, in units of $(mm/sec^2)^2$), b: coherence, c: phase spectrum. The mechanical peak frequency estimated from the phase spectrum is 7.4 ± 0.2 is not consistent with that estimated from the ACC power spectrum of 6.2 ± 0.1.

Fig. 5 Coherency spectra between the EMG time series recorded from the left and right side of the body. The horizontal line displays the confidence level s of Eq. (13). (A) Three control subjects, (B) Subjects with persistent mirror movements (PMM). The confidence level for zero coherence at the level of 5% is marked.

Fig. 6 (a) Schematic layout of the 42 EEG electrodes we analyzed. (b)-(f) Isocoherence maps for patients with an unilateral Parkinsonian tremor for the peak frequency of the tremor. The respective region showing the highest coherence is always contralateral to the trembling limb. The peak frequencies are (b): 4.9 Hz., (c) 4.6 Hz., (d) 4.8 Hz., (e) 5.6 Hz., (f) 4 Hz.

Fig. 7 Isocoherence maps for a healthy subject during enforced oscillation of the left hand. For the color scale and the assignment of the electrodes, see Fig. 6.

Fig. 8 Spectra (a,d,f), conventional (dotted lines) and partial (solid lines) coherence spectra (b,c,e) for the left hand extensor EMG and the EEG channels P1 and C2P. The spectra are displayed on logarithmic scale. The simultaneous confidence levels for zero partial coherence at the 5% level are marked.

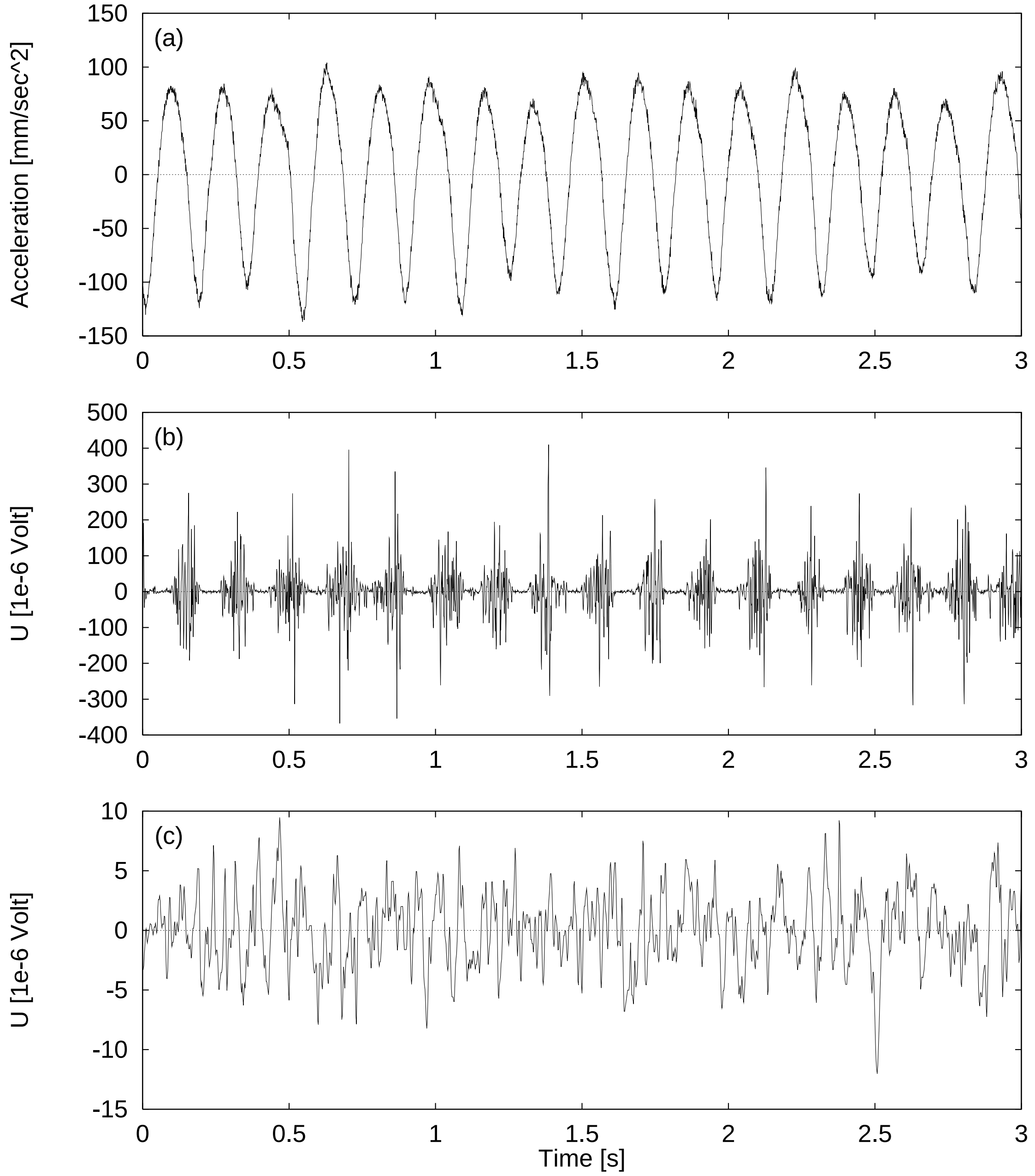

Figure 1: J. Timmer

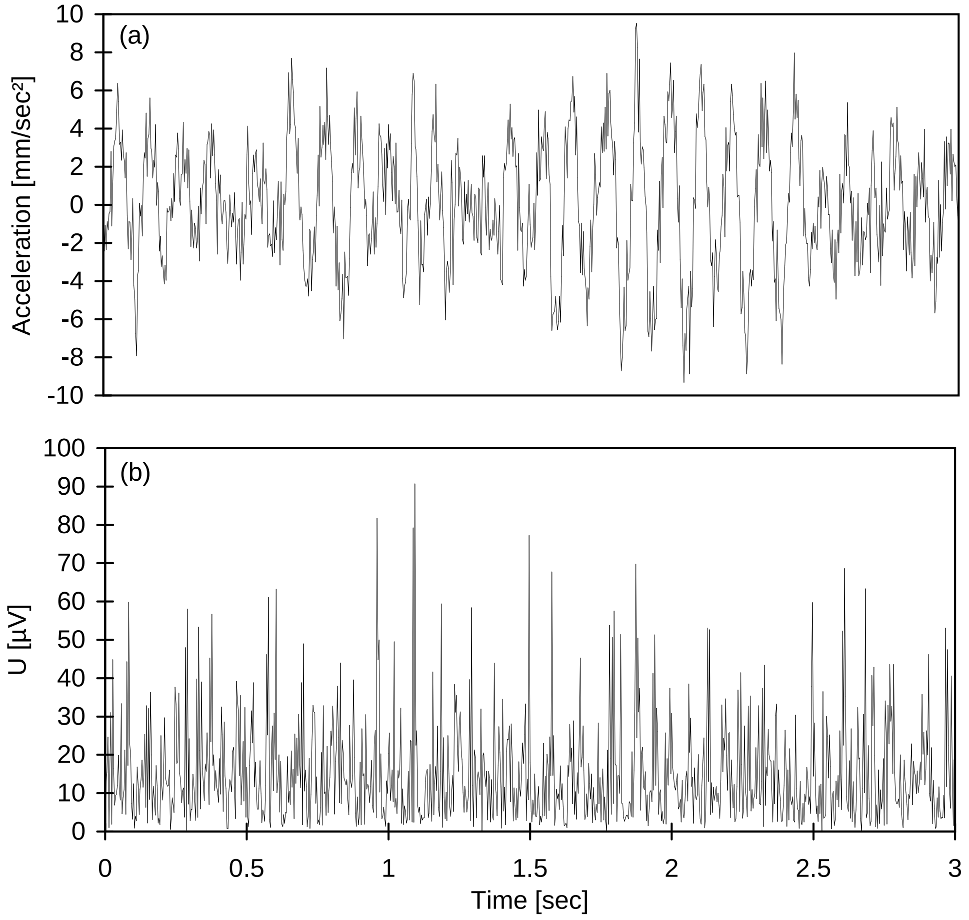

Figure 2: J. Timmer

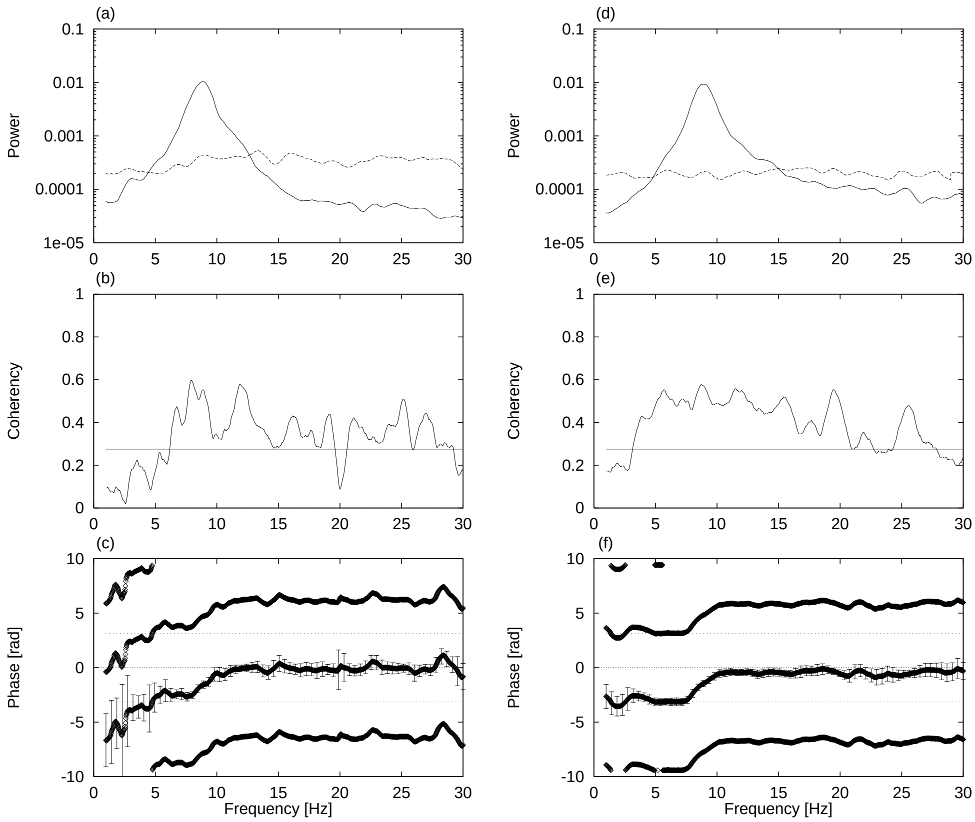

Figure 3: J. Timmer

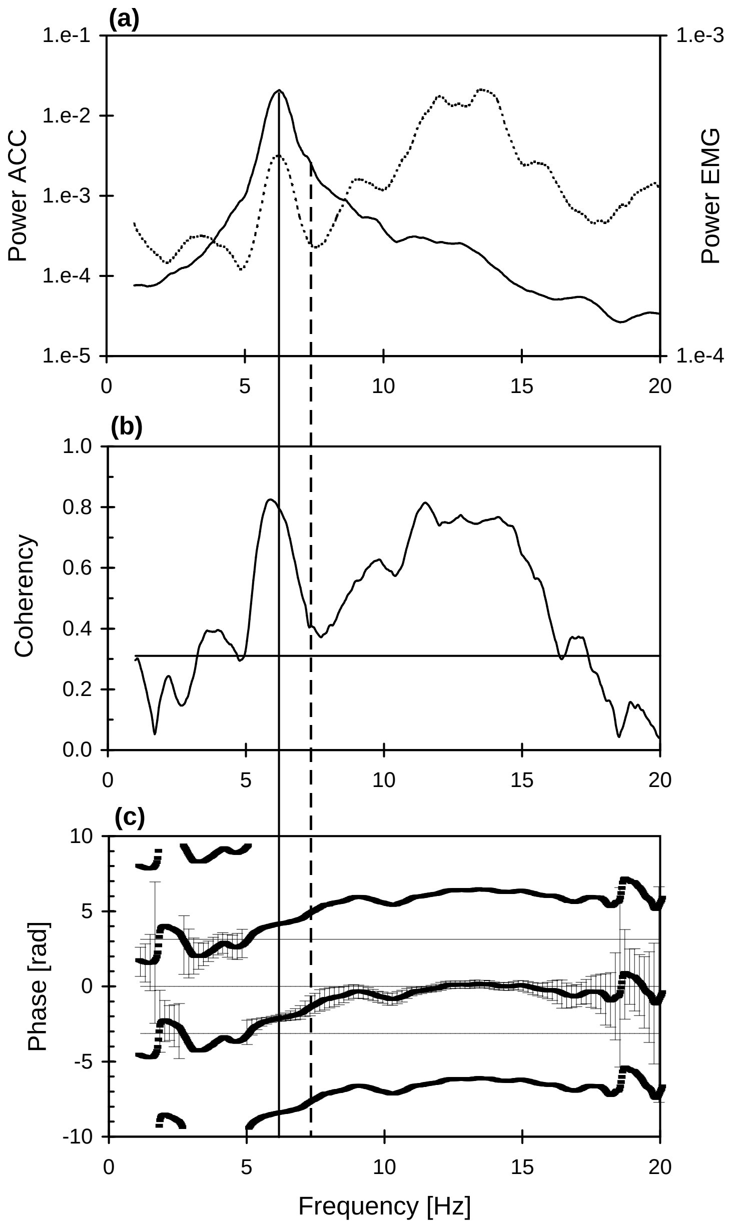

Figure 4: J. Timmer

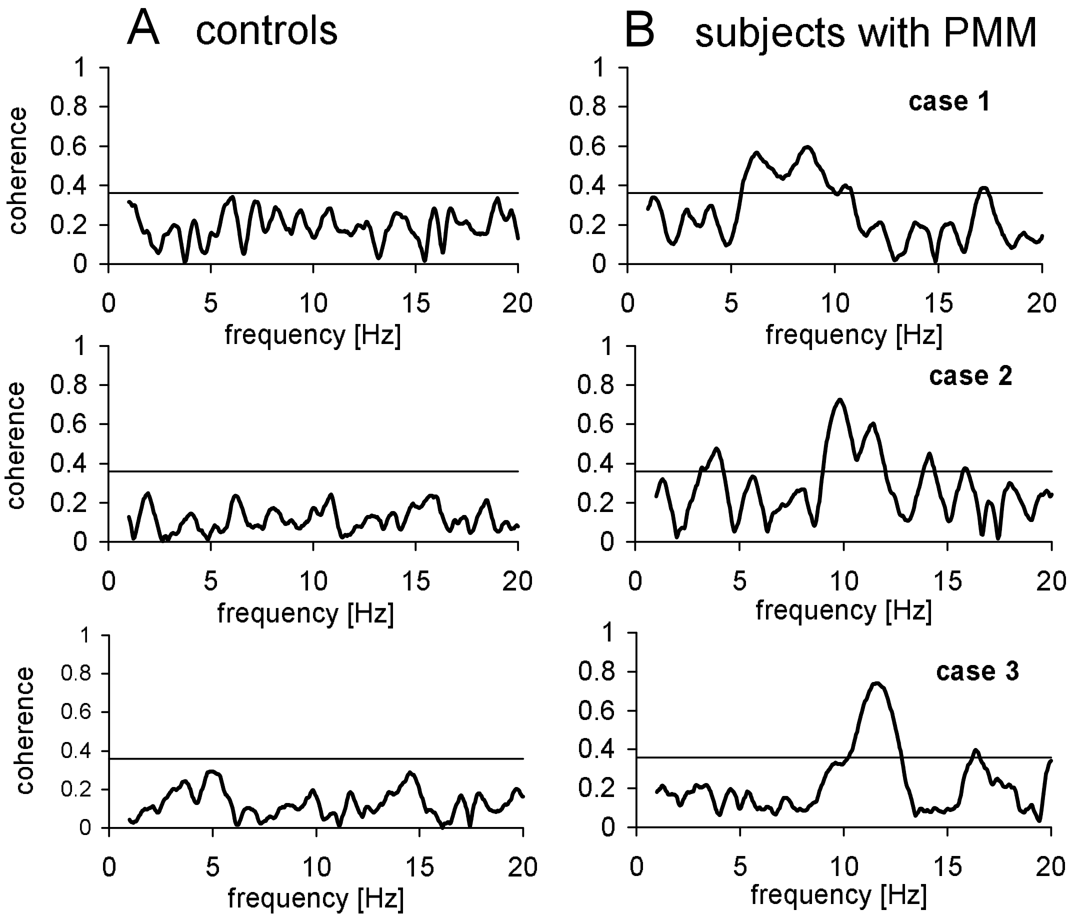

Figure 5: J. Timmer

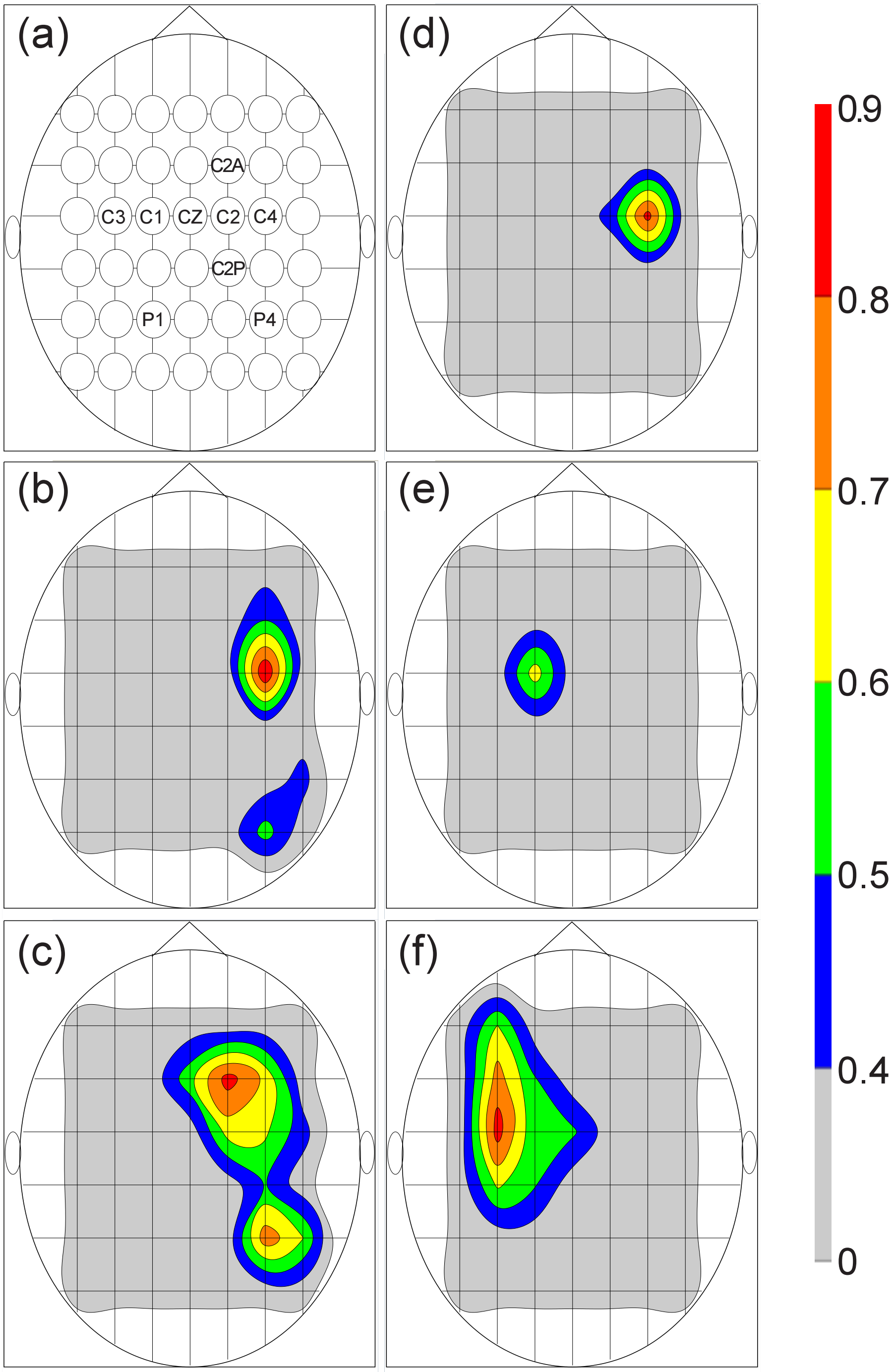

Figure 6: J. Timmer

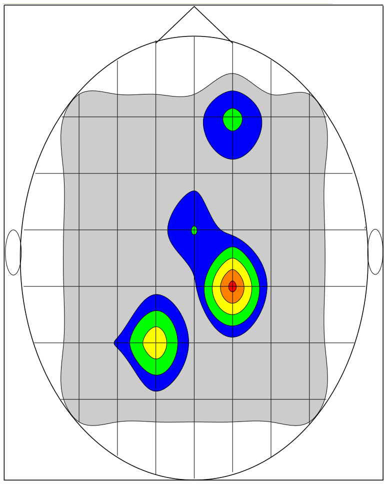

Figure 7: J. Timmer

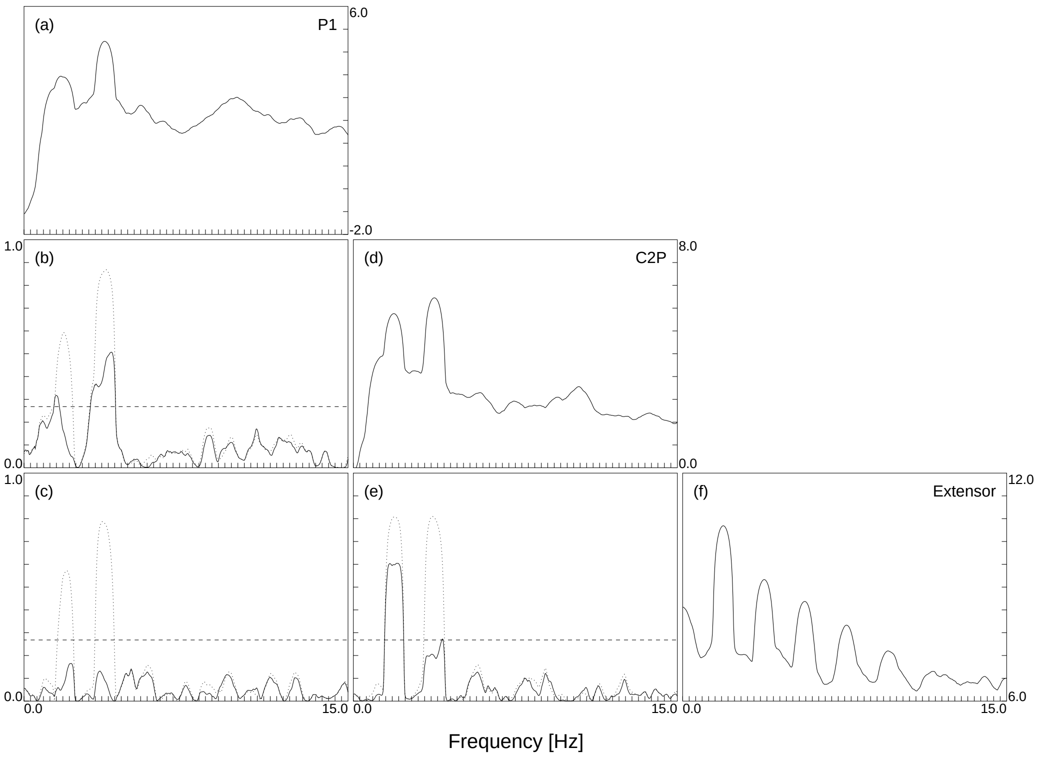

Figure 8: J. Timmer